1993
GROUND WATER
MODELING CONFERENCE

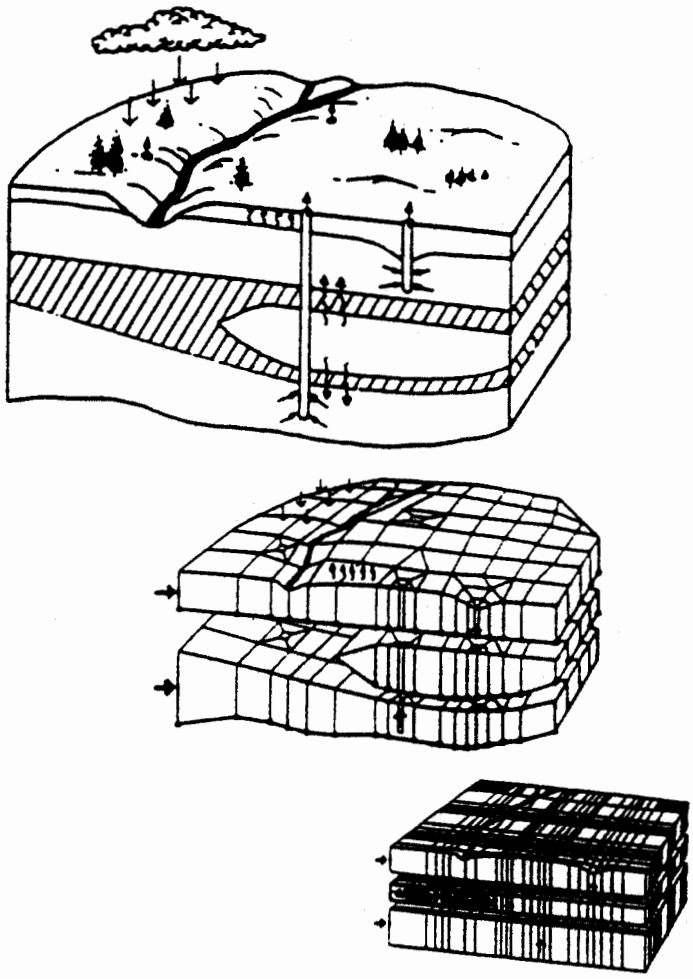

June 9-12, 1993
Colorado School of Mines Campus
Golden, Colorado

igwmc
international ground water modeling center

SCHOOL OF MINES 1874 COLORADO

PROCEEDINGS

1993
Ground Water
Modeling Conference

June 9-12, 1993
Colorado School of Mines Campus
Golden, Colorado

Sponsored by

The International Ground Water Modeling Center of the Colorado School of Mines

in cooperation with
Special Programs and Continuing Education of the Colorado School of Mines and Environmental Education Enterprise Institute

1993 Groundwater Modeling Conference

Proceedings of the Groundwater Modeling Conference
Golden, Colorado, June 9-12, 1993.
Organized by the International Ground Water Modeling Center (IGWMC)
at the Colorado School of Mines

Edited by:

E. Poeter
Dept. of Geology & Geological Engineering
Golden, Colorado

S. Ashlock
Special Programs and Continuing Education
Golden, Colorado

J. Proud
Special Programs and Continuing Education
Golden, Colorado

Copyright 1993 by
Colorado School of Mines

Printed in the United States of America

All rights reserved. This book, or parts thereof, may not be reproduced in any form without permission of the publisher.

Library of Congress Catalog Card Number
ISBN 0-918062-85-3

Conference Organizing Committee

Conference Chairperson
Eileen Poeter
Colorado School of Mines

Laj Ahuja
U.S. Dept. of Agriculture-ARS

Darcy Campbell
U.S. Environmental Protection Agency

Mary Hill
U.S. Geological Survey

Tissa Illangasekare
University of Colorado

Catherine Kraeger-Rovey
W&EST

Mary Pigman
International Ground Water Modeling Center

Richard Ribbens
U.S. Bureau of Reclamation

Judith Schenk
Office of Surface Mining

Peter Siton
Dames & Moore

Paul van der Heijde
International Ground Water Modeling Center

James Warner
Colorado State University

MODELING THE INTERACTION OF SORPTION AND BIODEGRADATION ON TRANSPORT IN GROUND WATER *IN SITU* BIOREMEDIATION SYSTEMS

Joseph E. Odencrantz[1], Albert J. Valocchi[2] and Bruce E. Rittmann[3]

[1] Levine–Fricke, Inc., Engineers, Hydrogeologists and Applied Scientists, 1920 Main Street, Suite 750, Irvine, CA 92714

[2] University of Illinois at Urbana–Champaign, 2527 Hydrosystems Laboratory, 205 N. Mathews, Urbana, IL 61801

[3] Northwestern University, A228 Technological Institute, 2145 Sheridan Road, Evanston, IL 60208

ABSTRACT

Numerical experiments examining the effect of linear equilibrium adsorption of the electron donor and its subsequent effect on the biodegradation rate gave new insight on the behavior of homogeneous systems. Two regions of behavior, an initial rapid growth period (Region 1) and a long–term pseudo–steady–state (Region 2), were identified in the numerical experiments for the one–dimensional homogeneous system. The Region 2 long–term pseudo–steady–state cyclic phenomenon was examined in detail in order to determine the cause of this behavior. In the absence of significant biological growth, the injected electron acceptor front travels faster than the retarded electron donor front. This overlap leads to a region of simultaneously high electron donor and acceptor, which leads to biomass growth. Biodegradation utilizes the electron donor and acceptor, which results in a speed up of the retarded electron donor front and a slow down of the electron acceptor front until biomass growth peaks. This separation of the fronts diminishes the region of simultaneously high electron donor and acceptor, resulting in biomass decay. The resultant cyclic phenomenon is thus explained based upon the results of numerical experiments and to date has not been reported in the literature.

The lag time to the onset of Region 1 behavior increased as a result of increased sorption and decreased advection of the electron donor, which results in a decreased electron acceptor flux into the system due to increased biological growth. As the retardation factor of the electron donor increases in the experiments, the rate of biodegradation of the electron donor also increases. This is caused by the "reservoir" effect with increasing sorption of the electron donor, which is augmented further by increasing overlap of the electron donor and electron acceptor fronts. For a retarded electron donor, decreasing flow velocity increases the biodegradation rate in Region 1, and this effect is due to increasing the overlap of the electron donor and acceptor within the domain.

INTRODUCTION

Because of the high solid–water interfacial area of natural porous media, sorption is an important process governing the transport of organic compounds. Sorption retards the advective transport velocity of the organic compound, which usually is the electron donor. However, since most electron acceptors are not retarded, the advective velocity of the electron donor may be less than that of the electron acceptor. For cases typical of *in situ* bioremediation, in which the electron acceptor is injected into a contaminated groundwater plume, retardation can cause greater mixing between the migrating fronts, thus increasing the potential for simultaneously high concentrations of electron donor and electron acceptor and for enhanced biological activity .

The overall objective of this paper is to examine the influence of sorption upon coupled transport and biodegradation processes in one dimension. To better understand and evaluate the important phenomena related to sorption and biodegradation in homogeneous systems, the following two specific objectives are considered:

1. Examine in detail the effect of linear equilibrium retardation of the electron donor of the dual–substrate system undergoing biodegradation and transport processes in a homogeneous porous medium.
2. Determine the effect of velocity and sorption upon the mass of electron donor biodegraded in a dual–substrate system.

DETAILED EXAMINATION OF THE INTERACTION OF BIODEGRADATION AND SORPTION

The objective of this section is to identify the effects that retardation of the electron donor have when electron acceptor is input into a system containing background contamination of electron donor. We examine in detail the important interacting phenomena that occur in these complicated systems. Computer simulations were carried out with the physical and biological parameters used for the dual–substrate transport problem shown in Figure 1. In order to examine the influence of retardation, transient simulations were performed at a pore–liquid velocity of 0.10 m/day, and with the electron donor having a retardation factor equal to 3.

The problem of interest in this paper relates to the coupling of advection, dispersion, and biological reaction simultaneously for the electron donor, electron acceptor, and total biomass. In this case, the coupled governing mass balance equations are:

$$\frac{\partial S}{\partial t} = - v_x' \frac{\partial S}{\partial x} + \frac{\partial}{\partial x} D_x' \frac{\partial S}{\partial x} - R_S \tag{1}$$

$$\frac{\partial A}{\partial t} = - v_x \frac{\partial A}{\partial x} + \frac{\partial}{\partial x} D_x \frac{\partial A}{\partial x} - R_A \tag{2}$$

$$\frac{\partial M_T}{\partial t} = R_M \tag{3}$$

where S is the aqueous–phase concentration of electron donor, A is the aqueous–phase concentration of electron acceptor, M_T is the total biomass concentration, v_x is the average linear velocity, D_x is the hydrodynamic dispersion tensor, (v_x' and D_x' denote v_x/R_{fS} and D_x/R_{fS}, respectively, where R_{fS} is the retardation factor of the electron donor), R_S and R_A are biodegradation kinetic loss terms for S and A, respectively, and R_M is the net growth are of the biomass. The above equations are solved using a numerical technique called "operator splitting", the details of which can be found in Odencrantz et al. (1990). The kinetic terms R_S, R_A, and R_M are presented below.

The multiplicative Monod model has been applied to biodegradation modeling in groundwater by MacQuarrie et al. (1990) and Odencrantz (1992). The reaction rates for the electron donor and electron acceptor, as well as for the biomass, are given by the following equations.

$$R_S = \frac{M_T q_{mS}}{R_{fS}} \left(\frac{S}{K_s + S}\right)\left(\frac{A}{K_A + A}\right) \tag{4}$$

$$R_A = \gamma M_T q_{mS} \left(\frac{S}{K_s + S}\right)\left(\frac{A}{K_A + A}\right) = \gamma R_S \tag{5}$$

$$R_M = Y_S M_T q_{mS} \left(\frac{S}{K_s + S}\right)\left(\frac{A}{K_A + A}\right) - b M_T + b M_{To} \tag{6}$$

where q_{mS} is the maximum specific rate of substrate utilization of the electron donor, K_S and K_A are the half–velocity coefficients of the electron donor and acceptor, respectively, γ is a stoichiometric coefficient (mass A/mass S), b is the microbial decay coefficient, M_{To} is the background concentration of bacteria, and Y_S is the yield coefficient for the electron donor.

Figure 2 shows the normalized mass of electron donor biodegraded for a 100 day simulation. The mass is normalized by the retardation factor of the electron donor. Two computer simulations, one reactive and the other nonreactive, were required to generate the curve shown in Figure 2. In

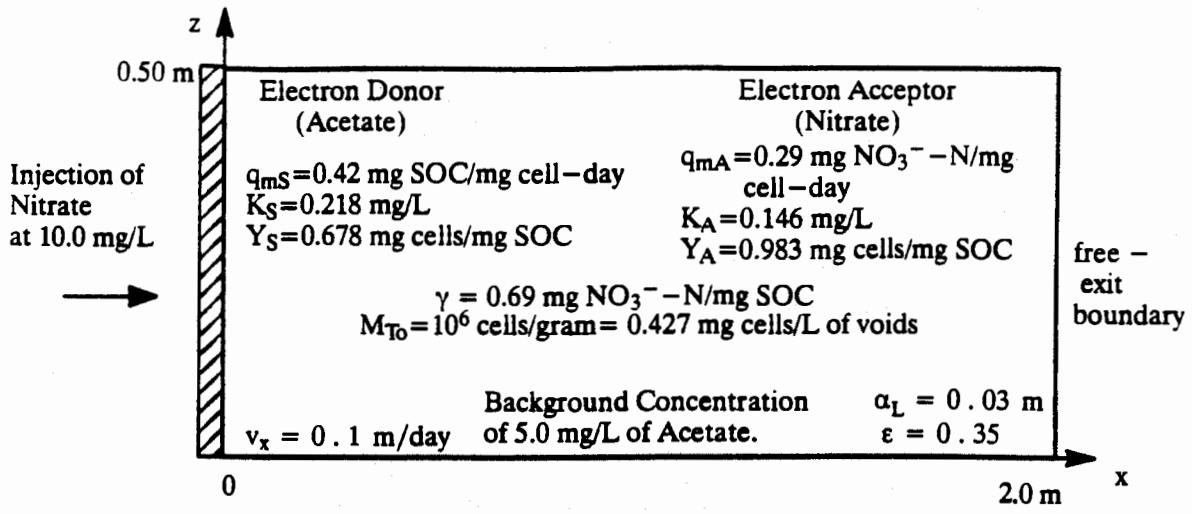

Figure 1. Domain and parameters used for the numerical experiments.

each simulation, the total mass of electron donor present (in the sorbed and dissolved phases) in the system at any particular time was computed by numerically evaluating

$$M_S(t) = \int_0^{L_x} \int_0^{L_z} \varepsilon \, R_{fS} \, S(x,z,t) \, dzdx \qquad (7)$$

Therefore, the total mass of electron donor biodegraded equals the difference between $M_S(t)$ in the nonreactive and reactive simulations; this quantity divided by R_{fS} is what is plotted on the ordinate of Figure 2. However, as the electron donor front migrates out the downstream boundary of the domain, the mass biodegraded is underestimated by this method, because the nonreactive simulation "loses" greater mass by advection out of the system than does the reactive simulation. The curve plotted in Figure 2 reaches a maximum value at day 85, where the electron donor begins to wash out of the system. Therefore, the curves illustrate the change in the mass of electron donor biodegraded only prior to the beginning of washout.

Two different, approximately linear−sloped regions can be defined; these are denoted Regions 1 and 2 in Figure 2. The slopes of Regions 1 and 2 are 181 mg/day and 85.5 mg/day, respectively. As will be discussed further, these two regions are indicative of an early−time rapid growth period and a long−term quasi−steady state. The Region 2 curve also displays a mild cyclic behavior about the mean of the linear trend indicated by the dashed line in Figure 2. Longitudinal profiles of the electron donor, electron acceptor, and biomass at selected times help explain these two different regions in detail.

Snapshots of the electron donor, electron acceptor, and biomass at eight times are shown in Figure 3. The peculiar shape of the electron acceptor front at day 15 is the result of increased electron−acceptor utilization due to rapid biomass growth in the vicinity of the retarded electron−donor front. In the absence of degradation, the injected electron acceptor moves at a speed of 0.10 m/day, and the displaced electron donor front moves at a speed of 0.033 m/day. The forward "limb" of the electron acceptor profile at day 15 appears to be located at x = 1.5 m and, hence, corresponds approximately to nonreactive transport behavior. Due to continuing injection of electron acceptor, a region of enhanced biological activity develops in the vicinity of the retarded electron donor front. Most of the injected electron acceptor is utilized in this region. The snapshots of the biomass show that the greatest biomass growth occurs at the interface between the electron donor and electron acceptor fronts. The electron donor profile at day 25, during the transition from Region 1 to Region 2, has a slightly different shape from that at day 15. The profiles

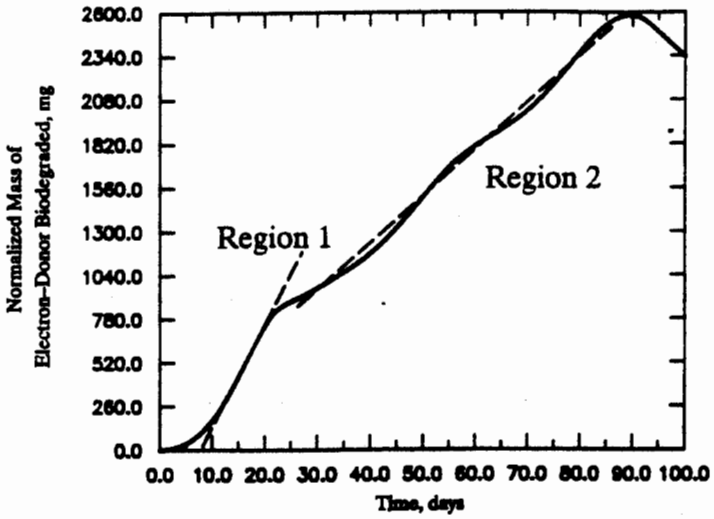

Figure 2. Mass of electron donor biodegraded for the simulation with the longer grid length with the retardation factor of 3 and v=0.10 m/day.

from day 35 to 75 vary slightly in shape and are shifted non-uniformly, which is consistent with the apparent cycling about the line drawn through Region 2 in Figure 2.

The snapshots of the electron acceptor in Figure 3 reveal the apparent upgradient retreat of the electron acceptor toward the vicinity of greatest biomass growth and indicate that different processes are taking place in Region 1 versus Region 2. The profile at day 25 is in the transition between Regions 1 and 2 and takes a shape more similar to the those in Region 2. The profiles within Region 2 again exhibit the apparent cyclic behavior in their shape and the spacing between them.

The snapshots of the biomass shown in Figure 3 show a change in the biomass profile shape after day 25. Biomass growth is rapid and concentrated in Region 1, but more spread out in Region 2. The biomass profiles in Region 2 again illustrate cyclic behavior. It is interesting to note the similarities between the profiles at days 45 and 75 and to carefully examine where these times fall within the cycles shown in Figure 2. They occur as the cycle moves above the average line. It appears that the fronts at days 45 and 75 correspond to the beginning and end of one approximately complete cycle. The cyclic behavior is illustrated quite clearly in the total amount of biomass curve shown in Figure 4.

In order to gain additional insight into the key difference between Regions 1 and 2 and the apparent cyclic phenomena characteristic of Region 2, normalized profiles of the electron donor, electron acceptor, and biomass at selected times are examined. The normalization of the electron donor and electron acceptor was performed by dividing the concentration values by the background and injection concentrations, respectively. The normalization of the biomass was performed by subtracting the background biomass concentrations from the biomass concentration values and dividing the difference by 5.024 mg/L, the maximum biomass concentration in Figure 3. Figure 5 shows the normalized profiles of the electron donor, electron acceptor, and biomass for days 15, 55, and 70. The profiles at day 15 are representative of Region 1 behavior. As discussed previously, the Region 1 behavior corresponds to the initial rapid growth phase. The electron-acceptor profile at day 15 is in the process of being "pinched off" by the intense biological reaction kinetics taking place. The peak of the biomass curve at 0.5 m coincides with the bend in the electron acceptor curve at approximately 1 meter into the domain. The key point is that all three profiles overlap quite a lot, especially near 0.9 m.

The normalized profiles of the three constituents at days 55 and 75 in Figure 5 demonstrate the cyclic behavior of Region 2. These times correspond to the maximum and minimum of the total biomass curve (Figure 4) within the same cycle. A maximum occurred at day 55 and a minimum at day 70 within the cycle bounded approximately by days 46 and 75, i.e. a 29-day cycle length. The

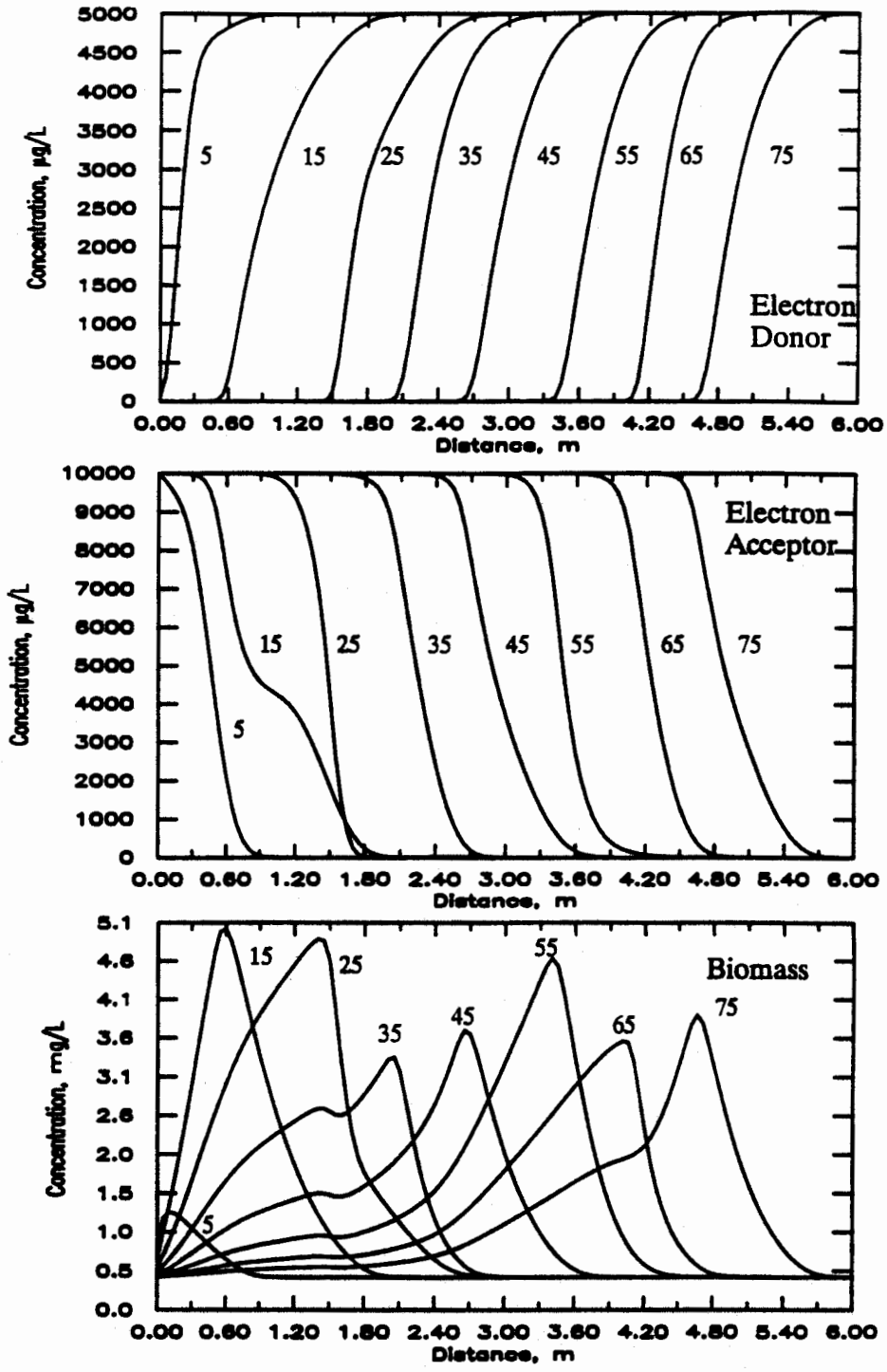

Figure 3. One-dimensional snapshots of the electron donor, electron acceptor, and biomass at the indicated times (days) for a retardation factor of 3 at a velocity of 0.10 m/day for the 6 m domain.

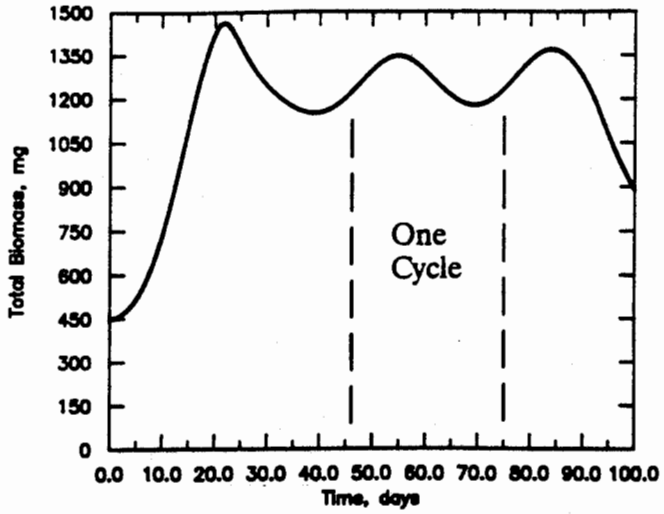

Figure 4. Total biomass in the system for a R_{fS} of 3 at a velocity of 0.10 m/day.

influence of dispersion and differential front speed (because the electron donor is retarded) is to mix the electron donor and electron acceptor plumes. But when mixing occurs, biological growth is induced, and the resulting utilization causes the fronts to sharpen and separate. This separation occurs because the utilization is greatest at the downstream portion of the electron acceptor front and the upstream portion of the electron donor front. Hence, the electron acceptor front slows down relative to the electron donor front, which speeds up. This is depicted at day 55 in Figure 5. But, because the region of electron donor and electron acceptor must overlap to have utilization, the growth diminishes, which causes the electron acceptor front to speed up relative to the electron donor. Then, overlap increases again, as shown at day 75 in Figure 5. This increased overlap causes increased biological activity, and the cycle begins again.

An interesting way to verify the cyclic behavior of Region 2 is to compare the normalized profiles at the beginning and end of the cycle defined by days 46 through 75. Theoretically, if the behavior is indeed cyclic, then the profiles at the end of a cycle should be a pure translation of those at the beginning. Figure 6 shows the normalized profiles of the electron donor, electron acceptor, and biomass for day 46, while Figure 7 shows the normalized profiles for day 75. We see that the profiles of the three constituents at days 46 and 75 are very similar in shape and magnitude. They are simply translated by 1.9 meters. Therefore, the hypothesis of the cyclic behavior with Region 2 is supported, and the cycle period is approximately 29 days. An average combined front speed of all three constituents can be determined by dividing the translated distance by the cycle period, i.e. 1.9 m/29 days. The value that results is 0.065 m/day. This implies that the average electron donor speed is approximately two times larger than the retarded pore–water velocity (0.033 m/day), while the average electron acceptor speed is approximately 0.65 times the pore water velocity (0.10 m/day).

In summary, when a nonsorbing electron acceptor is input into a system containing a background level of sorbing electron donor enhanced biological activity results due to the degree of overlap and mixing of the electron acceptor and donor. This results in a rapid initial growth phase, denoted Region 1. The increase in biomass leads to an increase in the utilization of the electron donor and acceptor; utilization is greatest at the downgradient portion of the electron acceptor front and the upgradient portion of the electron donor front. Hence, the fronts tend to separate, and the initial rapid growth decreases to a steady state growth phase, denoted Region 2. However, Region 2 exhibits some very interesting oscillations about its steady state; the nature of these oscillations were described in detail and are shown in Figures 5–7. The Region 2 behavior requires that the domain be long enough that the 'steady state' biomass can build up before the electron donor front washes out of the domain. It is conceivable that Region 2 could be totally missed if the modeling or laboratory experiments were conducted over small time–space scales.

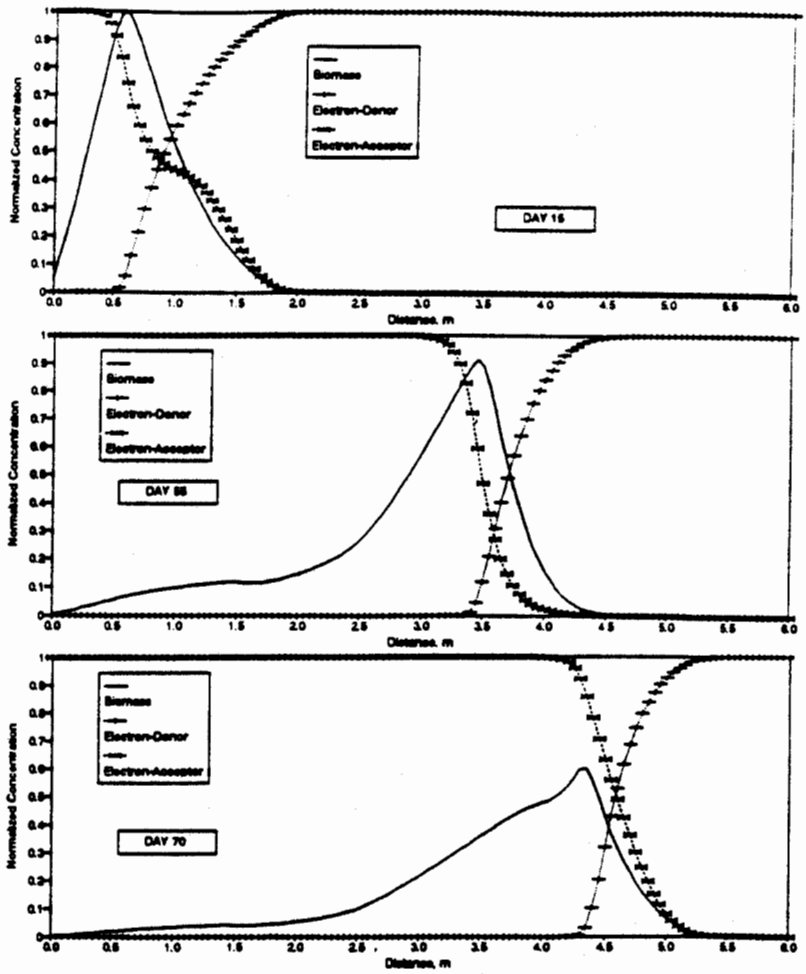

Figure 5. Normalized distribution of the electron donor, electron acceptor, and biomass at days 15, 55, and 70.

EFFECTS OF VELOCITY AND SORPTION PARAMETERS ON REGION 1 BIODEGRADATION

The effect of retardation of the electron donor is dependent upon many parameters that comprise the system. One of the most highly variable parameters is the velocity of the groundwater. Initial investigation into the effect of varying groundwater velocity and retardation coefficient was performed. The results of nine cases were examined. These nine transient experiments were conducted at three velocities (0.10, 0.55 and 1.0 m/day) and three retardation factors (R_{fS} =1, 3, and 10). The values of the retardation coefficients were selected in part by considering Chiang et al.'s (1989) finding of decreasing biodegradation with increasing adsorption when the retardation factor increased above three.

The lag time values are tabulated in Table 1, and the Region 1 biodegradation rates are reported in Table 2.The lag time values reported in Table 1 increase with greater R_{fS} and lower velocity. The increase in the lag time as a function of increasing R_{fS} illustrates that more retardation results in slowing down the initial biodegradation in the system. Chang and Rittmann (1987) reported this same behavior for bacterial growth on activated carbon. The increase in lag time for lower velocities can be understood better with the aid of the normalized lag time values

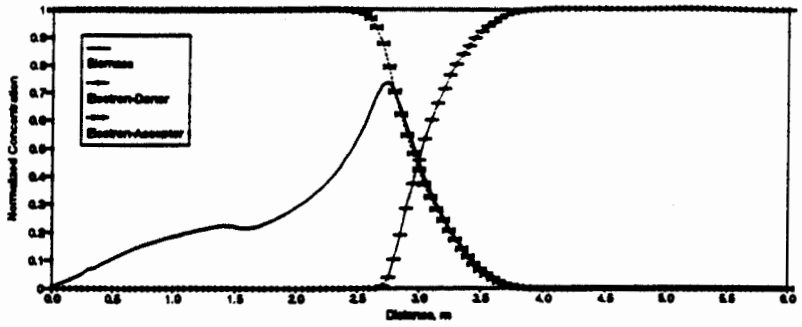

Figure 6. Normalized distribution of the electron donor, electron acceptor, and biomass at day 46, the beginning of a cycle.

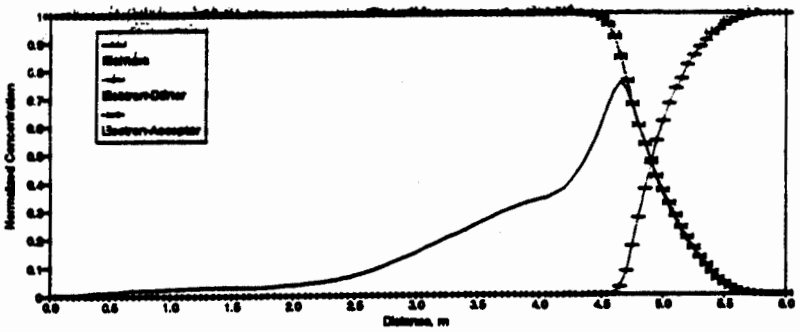

Figure 7. Normalized distribution of the electron donor, electron acceptor, and biomass at day 75, the end of a cycle.

shown in Table 1. The normalization of the lag time by R_{fS} shows that the lag time changes are approximately proportional to R_{fS}. The relatively constant values of normalized lag time with increasing R_{fS} shows that increasingly strong adsorption makes the substrate less available for initiating bacterial growth. The normalized lag times are inversely proportional to the flow velocity for a constant R_{fS}. This phenomena suggests that the flux of the electron acceptor also is limiting initiation of significant bacterial growth.

Table 1 Approximate Lag Times to Region 1 for the Three Different Velocities in the Homogeneous Numerical Experiments (Values in Parentheses are Normalized by R_{fS})

	Lag Time (days)		
R_{fS} v=	1.0 m/day	0.55 m/day	0.10 m/day
1	0.3 (0.3)	1.2 (1.2)	2.6 (2.6)
3	1.1 (0.37)	2.5 (0.83)	11.4 (3.8)
10	7.0 (0.70)	11.5 (1.15)	14.7 (1.47)

The trends with increasing retardation of the Region 1 biodegradation rate presented in Table 2 can be explained as follows. First, the absolute value of the linear biodegradation rate increases with increasing R_{fS} for a fixed velocity, but the normalized rates change much less dramatically. These results indicate that two effects are occurring. The first effect is that adsorption creates a "reservoir" of electron donor substrate. As aqueous phase electron donor is degraded, the sorbed phase substrates desorbs (instantly, because equilibrium is assumed). The sorbed phase, thus, is a

Table 2 Approximate Region 1 Biodegradation Rates of the Electron Donor for the Three Different Velocities in the Homogeneous Numerical Experiments (Values in Parentheses are Normalized by R_{fS})

	Rate of Biodegradation (mg/day)		
R_{fS} v=	1.0 m/day	0.55 m/day	0.10 m/day
1	28.4 (28.4)	29.5 (29.5)	23.6 (23.6)
3	57.3 (19.1)	72.6 (24.2)	181. (60.3)
10	214. (21.4)	619. (61.9)	510. (51.0)

source of substrate, and greater R_{fS} makes the reservoir of substrate greater. Having a greater reservoir of electron donor prolongs the extent of high electron–donor and –acceptor overlap, which leads to more significant utilization and growth.

If the reservoir of the electron donor were the only mechanism occurring, the normalized rate values would be approximately equal. However, the normalized rates generally increases with increasing R_{fS}. Thus a second mechanism appears to be acting. As R_{fS} increases, the speed of the electron–donor front decreases relative to that of the nonretarded electron acceptor. This results in a greater degree of overlap of the two fronts and, thus, a larger zone in which the electron donor and acceptor are simultaneously high, which leads to faster biological growth. While increased utilization of the electron acceptor causes its front to "retreat" (i.e. the electron acceptor front is "eaten" upgradient) desorption of the electron donor prevents utilization from "advancing" the electron donor front upgradient. Apparently, the increased front overlap augments the reservoir effect and (generally) allows the normalized biodegradation rate to increase with increasing R_{fS}.

For the case of a fixed retardation factor, it is necessary to examine the normalized biodegradation rates shown in Table 2. For $R_{fS}=1$, there is little front overlap because longitudinal dispersion is the only factor causing mixing between the electron–donor and –acceptor fronts. Therefore, the biodegradation rate is roughly constant with velocity. (Note, one could interpret the slight increase with velocity as reflecting the fact that longitudinal dispersion = $\alpha_L v$ increases with v). For $R_{fS}=3$ and 10, front overlap is enhanced due to retardation of the electron–donor front. In this case, a slow velocity allows the full front–overlap to develop within the 2–m grid and permits sufficient contact between the electron–donor and –acceptor that the biomass can grow rapidly. Therefore, for retarded cases, a velocity decrease increases the biodegradation rate within the 2–m domain. The result for $R_{fS}=10$, v=0.10 m/day is an anomaly to this trend, but this could be due to inaccuracies in estimating a Region 1 slope.

SUMMARY AND CONCLUSIONS

The importance of sorption processes in combination with transport processes and biodegradation kinetics was examined in a homogeneous system. More specifically, the linear equilibrium adsorption of the electron donor and its subsequent effect on the biodegradation rate gave new insight on the behavior of the homogeneous systems. Two regions of behavior, an initial rapid growth period and a long–term pseudo–steady–state, were identified in the numerical experiments for the one–dimensional homogeneous system. The apparent linear biodegradation rate of the electron donor for the initial rapid growth period also was determined for a series of different retardation factors and velocities. As the retardation factor increased, the Region 1 biodegradation rate also increased.

The following specific conclusions can be drawn from the results of the numerical experiments of transport and biodegradation in homogeneous and stratified porous media presented in this chapter.

1. The results of the experiments revealed two different linear regions, which correspond to an initial rapid growth phase (Region 1) and then a long–term pseudo steady–state of the electron donor, electron acceptor, and biomass profiles (Region 2).
2. The Region 2 cyclic phenomenon was examined in detail in order to determine the cause of this

behavior. In the absence of significant biological growth, the injected electron acceptor front travels faster than the retarded electron donor front. This overlap leads to a region of simultaneously high electron donor and acceptor, which leads to biomass growth. Thus, overlap of the electron donor, electron acceptor, and biomass profiles is required in order to achieve substantial biodegradation. But, biodegradation results in utilization of electron donor and acceptor, which results in a speed up of the retarded electron donor front and a slow down of the electron acceptor front. This separation of the fronts diminishes the region of simultaneously high electron donor and acceptor, resulting in biomass decay.

3. The lag time to the onset of Region 1 behavior increased as a result of increased sorption and decreased advection, which results in a decreased electron acceptor flux into the system due to increased biological growth.

4. As the retardation factor of the electron donor increases in the homogeneous experiments, the rate of biodegradation of the electron donor also increases. This is caused by the "reservoir" effect with increasing sorption of the electron donor, which is augmented further by increasing overlap of the electron donor and electron acceptor fronts. For a retarded electron donor, decreasing flow velocity increases the biodegradation rate in Region 1, and this effect is due to increasing the overlap of the electron donor and acceptor within the domain.

ACKNOWLEDGEMENTS

The research described in this article was supported by the U. S. Department of Energy, Office of Energy Research, Ecological Research Division and by Battelle Pacific Northwest Laboratory. This paper has not been subjected to either agency's peer or administrative review and therefore does not necessarily reflect the views of the agencies and no official endorsement should be inferred.

REFERENCES

Chang, H. T. and B. E. Rittmann. 1987. "Verification of the Model of Biofilm on Activated Carbon." Environ. Sci. Tech., Vol. 21, No. 3: 280–288.

Chiang, C. S., C. N. Dawson, and M. F. Wheeler. 1989. "Modeling of In–Situ Biorestoration of Organic Compounds in Groundwater." Transport in Porous Media, Vol. 6:667–702.

Odencrantz, J.E., A.J. Valocchi, and B.E. Rittmann. 1990. Modeling Two–Dimensional Solute Transport With Different Biodegradation Kinetics. Proceedings of the Fourth Annual Petroleum Hydrocarbons and Organic Chemicals in Ground Water Conference. NWWA/API: 355–368.

Odencrantz, J.E. 1992. Comparison of Minimum–Rate and Multiplicative Monod Biodegradation Kinetic Models Applied to In Situ Bioremediation. Proceedings of the Solving Ground Water Problems with Models Conference. IGWMC. pp. 479–493.

MacQuarrie, K. T. B., E. A. Sudicky, and E. O. Frind. 1990. "Simulation of Biodegradable Organic Compounds in Groundwater, 1, Numerical Formulation in Principal Directions." Water Resources Research, Vol. 26, No. 2: 207–222.